IEEE Open Journal of
Power Electronics

Received 3 August 2020; revised 30 August 2020; accepted 4 September 2020. Date of publication 15 September 2020; date of current version 30 September 2020.

Digital Object Identifier 10.1109/OJPEL.2020.3024030

Modular ON/OFF and Phase-Shifting for High-Speed Radio Frequency Power Modulation

KAWIN SURAKITBOVORN (Student Member, IEEE), AND JUAN M. RIVAS-DAVILA (Senior Member, IEEE)

Electrical Engineering Department Stanford Univerisity, Stanford, CA 94305 USA

CORRESPONDING AUTHOR: KAWIN SURAKITBOVORN (e-mail: north@stanford.edu)

ABSTRACT Radio frequency (RF) power amplifiers are an integral part of many academic, medical, and industrial applications. For many of these applications, the RF power needs to quickly transition from one level to another. For switched-mode amplifiers, one way to achieve this is with an out-phasing modulation technique. This power control technique, however, presents its own disadvantages, including poor light-load efficiency and an increase in overall system size. In this paper, we present an alternative power modulation method to create a high-efficiency high-speed RF amplifier system. This control technique utilizes two mechanisms, modular on/off and phase-shifting. In modular on/off, a different number of sub-circuits are turned "on" or "off" to crudely adjust the output power. In phase-shifting, the smallest sub-circuit of the whole system is phase-shifted away from the rest of the circuit to fine-tune the output power. This system's performance is first compared with existing out-phasing systems via circuit simulation. Then, an actual circuit implementation with a 13.56-MHz, 1500-W RF amplifier is demonstrated. A 93% dc-to-RF efficiency is achieved at full load, and above 80% efficiency is maintained all the way down to 7% load.

INDEX TERMS Power combining, class-E amplifier, RF power amplifier, RF generator, RF power control, out-phasing, multi-level pulsing, Chireix.

I. INTRODUCTION

Radio frequency (RF) power amplifiers (PAs) are employed in many applications, ranging from RF communication, medical imaging, industrial plasma generation and processing, etc. Traditionally, linear amplifiers such as class-A, class-B, or class-AB are used because of their design simplicity and linearity. However, as the need for higher efficiency arises, switched-mode designs such as class-D [1]–[3], E [4], [5], F [6]–[8], E/F [9], Φ [10]–[12], etc. have risen in popularity. Unlike in a linear PA where the output power can be controlled with the RF input voltage amplitude, switched-mode design only outputs one power level at a given dc input voltage. To adjust the switched-mode PAs' output power, separate dc-to-dc converters are typically added to their front ends.

Depending on the specific application, the power amplifiers can have vastly different requirements in terms of power level, efficiency, linearity, transient response, etc. For example, in plasma etching applications, pulsed operations are highly advantageous [13]–[15]. Therefore, PAs designed for such applications must have high (kilowatts level) power, fast transient, and be capable of pulsed operations. To generate a single-level pulsing, one can rapidly turn switched-mode amplifiers on and off. However, this pulsing method is not viable for more complicated pulsing schemes such as multi-level pulsing [16]–[18]. For switched-mode PAs to switch between power levels, their front end dc-to-dc converters need to rapidly change the dc voltages. With up to 100 kHz pulse frequency demanded by the plasma industries, this translates to sub-microsecond transient time needed to switch from one voltage level to another. Even with specially designed dc-to-dc converters operating at megahertz frequency, this is still a challenging task.

One possible method to quickly adjust the output power of switched-mode PAs is outphasing or linear amplification with nonlinear components [19], [20]. In conventional outphasing, two constant-amplitude RF signals are added with a power combiner network. Then, the output power is controlled by the phase difference between the two power signals. With an

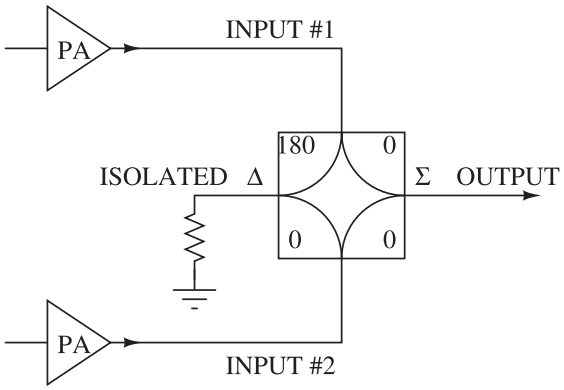

FIGURE 1. A typical isolating power combiner circuit consists of 2 input ports, 1 output port, and 1 isolated port.

isolating combiner, shown in Fig. 1, the mismatched portions of the input powers are isolated out and dissipated away as heat on an isolation resistor [21]. This severely reduces the system efficiency at medium and light loads.

One way to improve the overall system efficiency is by replacing the isolated load with a rectifier circuit to recover the energy back [22]–[24]. Another approach is to use a lossless non-isolating combiner network where the isolation port is not needed, with the Chireix combiner being the most well-known [25], [26]. Nonetheless, at light load (large outphasing angles), the reactive loading seen by the switched-mode amplifiers with Chireix combiner becomes substantial. This causes the switches to lose zero-voltage-switching (ZVS) conditions resulting in reduced light load efficiency. Other non-isolating combiners with improved performance have since been proposed [27]–[29], with the multi-way combiner network proposed by Perreault [30] promising the best light load performance.

While these outphasing techniques enable switched-mode amplifiers to quickly adjust their output power without changing their dc input voltages, they also have drawbacks. Regardless of the type, a combiner network consists of inductors, capacitors, or transmission lines. Under operation, each of these components will present their associated loss due to parasitic resistances. Thus, even with perfectly in-phased inputs, a "lossless" combiner network is never truly lossless, causing the efciency at the combined output to always be slightly lower than the original efciency of each power amplier. Furthermore, even with combiner topologies designed to suppress reactive loading and maintain ZVS, the switches' conduction loss can still reduce the system light load efficiency. Moreover, for applications where space is limited or where weight is critical (e.g., RF communication for cell-phones and micro-satellite propulsion), these components do take up extra valuable space and add excess weight to the system. Lastly, for certain types of combiner networks, the number of combinable power ampliers must also follow a binary sequence (2N = 2,4,8,16...), limiting the design freedom.

In our previous work, we presented an alternative approach to the problem of power combining by offering a tuning

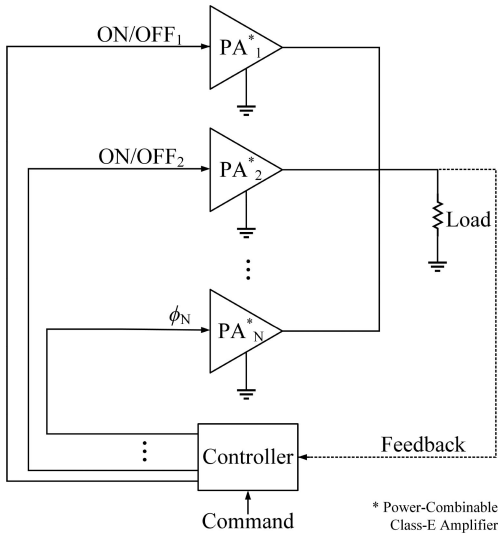

FIGURE 2. Top level diagram of the proposed control method. (Feedback design not discussed in this paper.)

method that allowed output powers from multiple amplifiers to be combined directly without the need for an extra power combiner network [31]. This eliminates the extra loss associated with the combiner network, reduces the system size and weight, as well as allows circuit designers the freedom to connect any number of power amplifiers together. In this paper, we offer a novel power control/modulation scheme shown in Fig. 2, suitable for this proposed direct combining circuit. This control technique requires no additional component to be added to the circuit. It allows arbitrary output power levels to be generated. It produces an extremely fast transient response when switching from one power level to another. More importantly, it achieves higher efficiency than any previously proposed outphasing system over the entire load range.

The outline of this paper is as follows. Section II summaries the proposed power combinable class-E amplifiers. Section III develops and analyzes the modular on/off control technique for discrete power levels generation in a system with multiple power combinable class-E amplifiers. Section IV presents a phase-shifting control technique that fills in the gap between the discrete power levels. Section V provides comparison between our proposed power modulation method and other known methods. Section VI showcases a multi-level 1500 W 13.56 MHz power amplifier design intended for plasma generation applications utilizing the proposed circuit and control technique. The system achieves a full load dc-to-RF efficiency of 93%, maintains efficiency above 80% down to 100 W, and takes less than 0.5 μs to switch from one power level to another. Finally, section VII concludes the paper.

II. SUMMARY OF THE TUNING FOR THE PREVIOUSLY PROPOSED POWER-COMBINABLE CLASS-E AMPLIFIER

The tuning for the power-combinable class-E amplifier was developed to allow multiple PAs to directly combine their

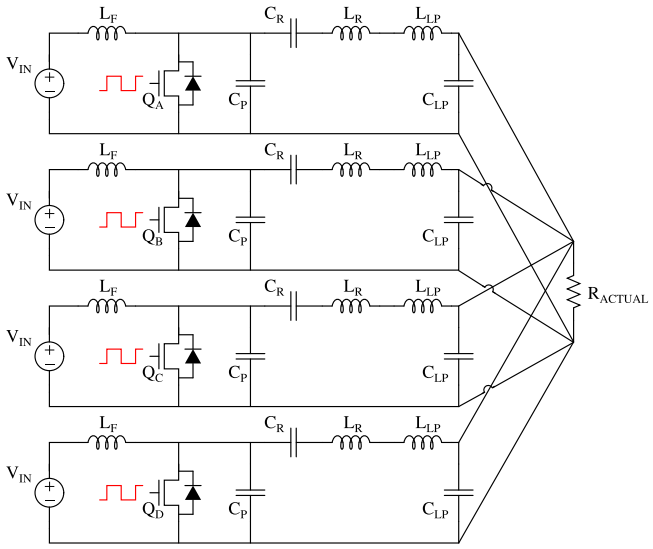

FIGURE 3. A system consists of 4 class-E amplifiers combining power at the output.

output powers without needing any extra components. The complete detailed analysis of this circuit is presented in [31].

Fig. 3 shows the schematic of multiple class-E amplifiers, each with a low-to-high LC matching network, directly connected at the output. We made the assumption that for most high power applications, the output impedance the amplifiers needed to see would be lower than the actual load impedance. As a result, a low-to-high matching network would be used as part of each amplifier circuit. Notice that there is nothing special about the circuit topology itself as the power combining capability actually comes from the selection of its component values described below, along with the control techniques presented in the later sections of this paper.

The tuning of power-combinable class-E amplifiers starts by selecting the component values, L_f, C_p, L_r, and C_r, as well as the output impedance each amplifier needs to see, R_o, following standard class-E design equations according to the desired operation regime and power level. For example, if one wishes to attain the maximum output power from a given switching device, according to Acar *et al.* [32], the following component values should be used:

$$R_o = \frac{k_p V_{\text{in}}^2}{P},\ C_p = \frac{k_c}{\omega R_o},\ L_f = \frac{k_l R_o}{\omega},$$
$$L_r = \frac{QR_o}{\omega},\ C_r = \frac{1}{\omega Q R_o},$$
$$(k_p = 1.365,\ k_c = 0.685,\ k_l = 0.732) \tag{1}$$

where Q is the desired loaded quality factor of the series output filter.

Depending on the required actual load impedance, R_{actual}, and the number of circuits to be combined, N, the load impedance each circuit has to be matched to, R_l, can be calculated from

$$R_l = N \times R_{\text{actual}}. \tag{2}$$

In order to minimize the effect one amplifier can have on the others, each matching network is modified to present a very high impedance looking in, effectively shielding each amplifier from the others, while still largely maintaining its impedance matching functionality. In the aforementioned paper, this condition is mathematically shown to be met when C_{lp} and L_{lp} values are tuned as follows

$$C_{lp} = \frac{1}{\omega\sqrt{R_l R_o}},\ L_{lp} = \frac{\sqrt{R_l R_o}}{\omega}. \tag{3}$$

This choice of C_{lp} and L_{lp}, however, makes the impedance looking into the modified low-pass network slightly inductive. For a class-E amplifier tuned according to (1) to achieve ZVS condition, an extra capacitance needs to be added to the C_p resulting in

$$C_{p,tot} = \frac{k_c}{\omega R_o}\left(1 + \sqrt{\frac{R_o}{R_l}}\right). \tag{4}$$

Lastly, it is also shown that with these modified matching network values, if the load resistance the amplifier sees were to change from $R_{l,\text{orig}}$ to $R_{l,\text{new}}$, the output power from that unit would then change to

$$P_{\text{out,new}} = P_{\text{out,orig}}\frac{R_{l,\text{new}}}{R_{l,\text{orig}}}. \tag{5}$$

III. MODULAR ON/OFF CONTROL TECHNIQUE FOR DISCRETE LEVEL OUTPUT POWER

This section will describe the modular on/off control technique and how it can be used to control the output power of the aforementioned circuit before mathematically analyzing its operation in detail.

A. CONCEPTUAL OVERVIEW

Looking back at the circuit in Fig. 3, from top to bottom, we will refer to each subcircuit as unit A, B, C, and D. When all four subcircuits are driven with the same gate signals, all four units will operate synchronously, and their output power will be combined across the R_{actual}, providing the full load power.

Next, let us look at what happens to the circuit operation when we stop providing gate signals to some of these switches. Those without gate signals will be referred to the "off" units, and those with gate signals as the "on" units. First, notice that with no gate signals, only the anti-parallel diodes of the switches are operative. As a result, these units now assume the topology of class-E rectifiers connecting to the fixed dc voltage, V_{in}. Depending on the amplitude of the RF output voltage across R_{actual}, two operation modes can happen. When the majority of the units are "on," the RF output voltage is high, and the "off" units operate as rectifiers converting some of the RF power back to dc, reducing the output power. Fig. 4 illustrates this mode of operation with three "on" units and one "off" unit.

As a larger part of the system is turned off, the RF power and the output voltage further reduces, causing the voltage across the diodes to become proportionally smaller. Since the

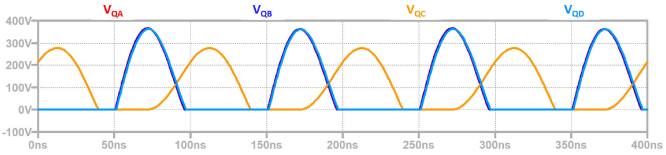

FIGURE 4. The drain waveforms of the simulated power-combinable class-E amplifier circuits under modular on/off control. In this case, unit A B and D (red/blue/light blue - overlapping waveforms) are driven normally and operate as amplifiers, while unit C (yellow) receives no gate signal and operates as a rectifier. Under this operation the output power is 392 W while the full power when all four units operate is 1000 W.

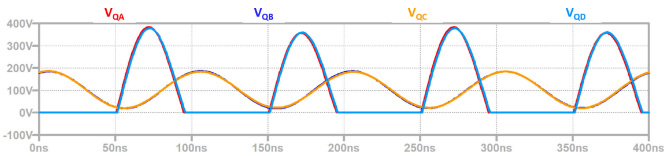

FIGURE 5. The drain waveforms of the simulated power-combinable class-E amplifier circuits under modular on/off control. In this case, unit A and D (red/light blue - overlapping waveforms) are driven normally and operate as amplifiers, while unit B and C (blue/yellow - overlapping waveforms) receive no gate signals and operate as resonant tanks. Under this operation, the output power is 201 W while the full power when all four units operate is 1000 W.

switches/diodes are connected to the fixed dc input voltage via $L_f(s)$, the RF voltages across them have to center around this dc voltage. Once these voltages' amplitudes are sufficiently low, their lowest points will be above zero, and the diodes will stop conducting altogether. Past this point, the "off" units will operate as resonant tanks, neither outputting RF power nor rectifying it back to dc. Fig. 5 illustrates this mode of operation with two "on" units and two "off" unit.

Consequently, by having N number of identical units combining power, this technique of turning "on/off" a different number of units can be used to generate N discrete levels of output power. For applications where discrete but predetermined output power levels are needed, a system could be designed around this control method to quickly achieve those power levels. Notice that while the relationship between the number of "on/off" units and the output power is monotonic, this relationship is not linear. To utilize this method of power control, the equations that relate the number of "on/off" units and the resulting output power are needed.

B. GENERAL CASE REPRESENTATION

To analyze this proposed control method in a more general term, we will first pretend that the system consists of infinitely many amplifiers combining power. While the notion of generating infinitely many power levels from an infinite number of amplifiers may seem unrealistic, achieving a large number of power steps is actually not difficult. Instead of designing all amplifiers for the same output power, if we were to tune each additional amplifier to output half the previous one's power, then 2^N discrete power steps can be generated from just N amplifiers. By designing the system this way, 256 discrete power levels can be generated with just eight amplifiers.

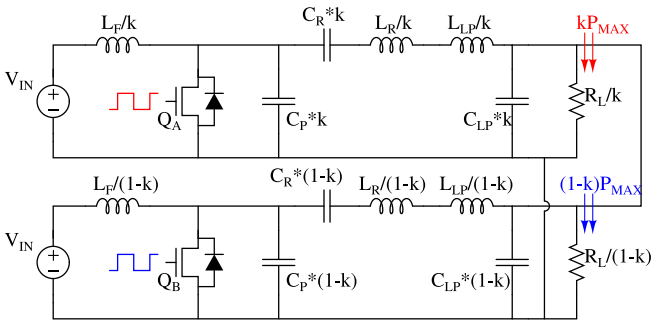

FIGURE 6. A circuit diagram representing the power-combined class-E amplifier with the portion k on top and the portion (1-k) on the bottom.

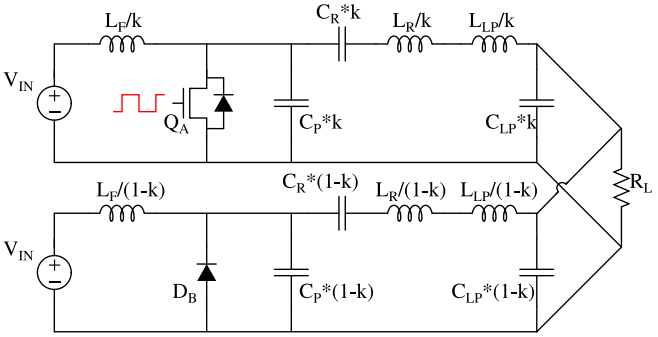

FIGURE 7. A circuit diagram representing the power-combined class-E amplifier with the portion k on top being driven and the portion (1-k) on the bottom not being driven.

With all units "on," the total combined output power is equal to $P_{\max}$. Fig. 6 represents this circuit. In this representation, the component values, $L_f, L_r, L_{lp}, C_p, C_r, C_{lp}$, and R_l are the combined component values from all the subcircuits. In other words, these values are calculated as if a single amplifier is designed to generate the full output power, $P_{\max}$. The circuit is then divided into two portions, with the k portion on top and the $(1-k)$ portion on the bottom. This number k can be any value between 0 and 1, and it represents the ratio of the output power from this k portion to the total output power when both portions are "on."

Using this notation, we can easily represent the overall circuit when a portion of it is not driven. Fig. 7 shows the same circuit but with the portion $(1-k)$ not driven. As a result, the switch Q_B can be ignored, leaving only the diode D_B operative. For example, in Fig. 4 with three out of four units "on," we have $k = 0.75$.

C. THE P_{out} VS k RELATIONSHIP

In modular "on/off" control, the term k, which represents the ratio of "on/off" units, serves as a handle to control the output power. Fig. 8 shows a typical P_{out} vs k relationship. This relationship is non-linear and is especially complicated around where the transition between the two previously mentioned modes of operation occurs. In real applications, the most practical way to get this exact relationship is via precise circuit simulations. Nonetheless, to better understand the proposed

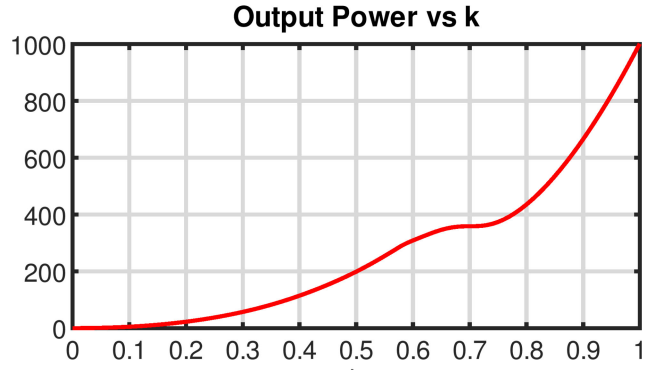

FIGURE 8. A typical relationship between the output power P_{out} [W] (y-axis) and the k term (x-axis).

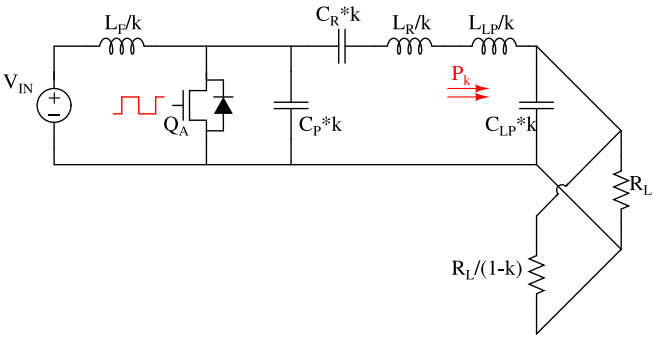

FIGURE 9. A simplified circuit diagram representing the power-combinable class-E amplifier under modular "on/off" control for the large k case.

circuit's operating principle and this control scheme, we will mathematically analyze the circuit at two limit cases. The first case is when k is close to 1 (a large portion of the circuit is driven), and the second case is when k is close to 0 (a large portion of the circuit is not driven).

1) THE LARGE k CASE

For the case where k is approximately larger than 0.75, the $(1-k)$ part of the circuit operates as a rectifier with close to 50% duty cycle. To facilitate the analysis, we will use the concept of time-reversal duality [33]. In Fig. 6, as an amplifier, the $(1-k)$ portion outputs its power to the load $R_l/(1-k)$. By invoking the time-reversal duality relationship, as a rectifier, the $(1-k)$ portion will then appear as an $R_l/(1-k)$ resistance to the rest of the circuit. Thus, in this large k case, the whole bottom part of the circuit in Fig. 7 can be replaced with an $R_l/(1-k)$ resistor.

In Fig. 6, with both portions driven, the k portion used to output $P_{\text{orig}} = kP_{\max}$ to a load $R_{\text{orig}} = R_l/k$. However, as shown in Fig. 9, with the $(1-k)$ portion now appearing as an $R_l/(1-k)$ resistor, the new load the k portion sees is

$$R_{\text{new}} = R_l // \frac{R_l}{(1-k)} = \frac{R_l}{(2-k)}. \tag{6}$$

From (5), the power-combinable class-E circuit's output power is linearly proportional to its load resistance. With the new load, the k portion will then output

$$P_k = P_{\text{orig}} \times \frac{R_{\text{new}}}{R_{\text{orig}}} \tag{7}$$

$$P_k = kP_{\max} \times \frac{k}{(2-k)}. \tag{8}$$

While this P_k is the output power from the k portion of the circuit, not all of it goes to the load R_l. The power that goes into the rectifier input impedance, $R_l/(1-k)$, will be converted back to dc, leaving only the R_{new}/R_l portion of the P_k to go toward the output load.

$$P_{\text{out}} = \frac{P_k}{(2-k)} = \frac{k^2}{(2-k)^2} P_{\max} \tag{9}$$

Fig. 10 compares this equation with the P_{out} vs k plot. It can be seen that the derived equation closely predicts the output power when k is large.

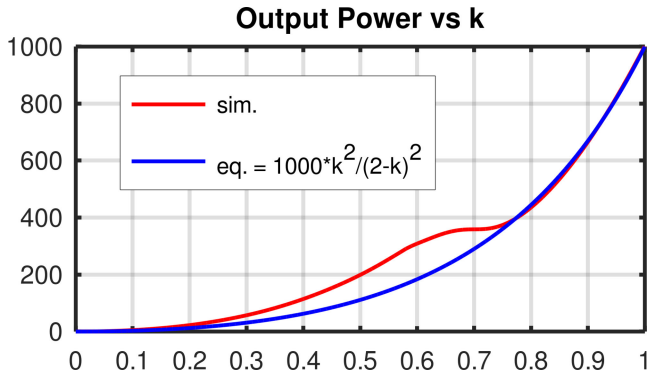

FIGURE 10. Comparison between the simulated (red) relationship between the k term (x-axis) and the output power (y-axis), and the derived equation (blue) for the large k case.

2) THE SMALL k CASE

When k is approximately less than 0.5, the output power at this modulation level is much lower than the full power. Low output power means that the voltage across the output load, as well as across the switch/diode of the "off" portion, will have small ac amplitudes. As explained in section III-A, since the voltage across the switch/diode of the "off" portion has to be centered around V_{in}, its lowest point will never get below zero when the ac voltage amplitude is sufficiently small. This causes the diode, D_B, to never conduct any current, virtually eliminated from the circuit.

In this mode of operation, by replacing the output voltage from the k portion with a sinusoidal voltage source at the fundamental frequency, we can simplify the circuit to Fig. 11. Here, the series-resonant filters appear as a short circuit and can be ignored. Moreover, the dc component can also be eliminated due to the dc-blocking effect of the series capacitors.

In this case, to calculate the output power, only the effective load impedance, Z_k, is needed. With this simplified circuit, Z_k

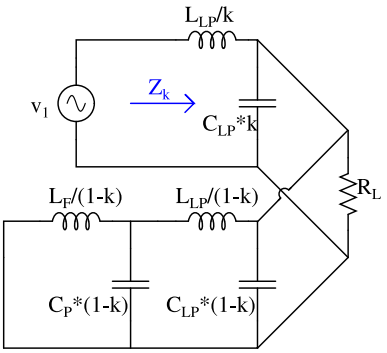

FIGURE 11. A simplified circuit diagram representing the power-combinable class-E amplifier under modular "on/off" control under the small *k* case.

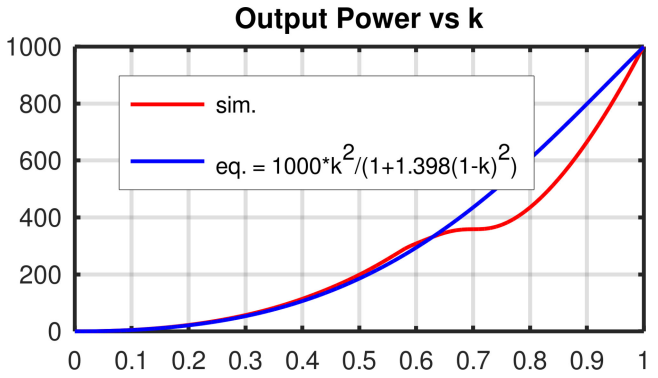

FIGURE 12. Comparison between the simulated (red) relationship between the *k* term (x-axis) and the output power (y-axis), and the derived equation (blue) for the small *k* case.

is calculated to be

$$Z_k = \frac{j\omega L_{lp}}{k} + \frac{R_l}{1 + j\omega C_{lp} R_l - \frac{j(1-k)R_l(1-\omega^2 L_f C_p)}{L_{lp}+L_f-\omega^2 L_f L_{lp} C_p}}. \quad (10)$$

Then, if the values for these components were selected according to equations in section II, it can be further shown that

$$Z_k = \frac{R_o}{k}\left[\frac{\sqrt{\frac{R_l}{R_o}}(1-k_l k_c)+k_l(1-k_c) + j\sqrt{\frac{R_l}{R_o}}k_l(1-k)}{k_l(1-kk_c)+\sqrt{\frac{R_l}{R_o}}(1-k_l k_c) - j(1-k_l k_c) - j\sqrt{\frac{R_o}{R_l}}k_l(1-k_c)}\right]. \quad (11)$$

As the $(1-k)$ portion only contains non-resistive passive components, the output power to the load is equal to the power from the $v_1 = Ve^{j(\omega t}$.

$$P_{\text{out}} = \mathbf{Re}\left[\frac{v_1 i_1^*}{2}\right] = \mathbf{Re}\left[\frac{v_1(v_1/Z_k)^*}{2}\right] = \frac{V^2}{2}\mathbf{Re}\left[\frac{1}{Z_k}\right] \quad (12)$$

By substituting in the Z_k and finding its real part, we can show that

$$P_{\text{out}} = \frac{V^2}{2R_o}\frac{k^2\left(\sqrt{\frac{R_l}{R_o}}(1-k_l k_c)+k_l(1-k_c)\right)^2}{\left(\sqrt{\frac{R_l}{R_o}}(1-k_l k_c)+k_l(1-k_c)\right)^2+\frac{R_l}{R_o}k_l^2(1-k)^2}. \quad (13)$$

Since $V^2/(2R_o)$ is the original un-modulated output power, we find that

$$P_{\text{out}} = \frac{P_{\max}\cdot k^2\left(\sqrt{\frac{R_l}{R_o}}(1-k_l k_c)+k_l(1-k_c)\right)^2}{\left(\sqrt{\frac{R_l}{R_o}}(1-k_l k_c)+k_l(1-k_c)\right)^2+\frac{R_l}{R_o}k_l^2(1-k)^2} = P_{\max}\cdot\frac{k^2}{1+C(1-k)^2}, \quad (14)$$

where C is a constant.

Fig. 12 compares this derived equation with the P_{out} vs k plot previously shown. As can be seen, the derived equation does a good job predicting the output power when k is small.

So far, we have a way to control the output power by turning "on/off" a different number of amplifiers. With infinitely many amplifiers, k can be of any value. Thus, any output power can be achieved according to the P_{out} vs k relationship. However, in real circuits, the term k can only take on discrete values. As a result, utilizing this method of power control alone will result in discrete output power levels. In the next section, a method to fill the gap between these discrete levels so that we can arbitrarily control the output power will be discussed.

IV. PHASE-SHIFTING CONTROL FOR ARBITRARY OUTPUT POWER

Here, we will describe the phase-shifting control technique and how it can be used to fill in the gap between resulting discrete power levels from the modular "on/off" control. To represent the general case under this control method, a new circuit notation will be used.

A. GENERAL CASE REPRESENTATION

Instead of dividing the circuit into k and $(1-k)$ portions, we will divide it into k, r, and $(1-k-r)$ portion. Fig. 13 shows the circuit diagram of this representation. Unlike in the previous section, we now assume that we only have a finite number of amplifiers. Thus, the term k can only take on a set of discrete values. The new term, r, is a single small value representing the proportion of the output power from this small unit that will be used as a knob in this control scheme. The gate signal to this portion is that from the portion k, but phase-shifted by θ. No gate signal is applied to the portion $(1-k-r)$. Again, under this description, the component values, L_f L_r L_{lp} C_p C_r C_{lp} and R_l are the combined component values of all the circuits.

B. CONCEPTUAL OVERVIEW

To illustrate the phase-shifting control, we will look at the case where, by design, our circuit can generate ten discrete power levels at ten evenly spaced k values with the modular "on/off" control alone. Table 1 shows an example of what these power levels could be.

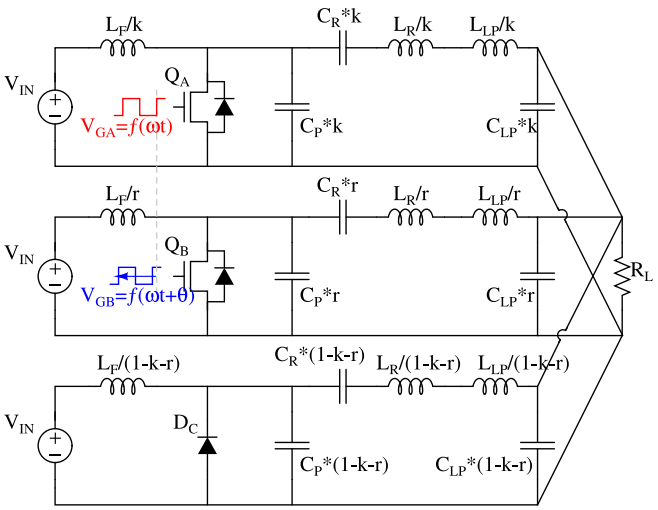

FIGURE 13. A circuit diagram representing the power-combined class-E amplifier for arbitrary output power. The portion *k* on top is driven by a fixed gate signal. The portion *r* in the middle is driven by a phase-shifted gate signal. The portion $(1 - k - r)$ on the bottom is not driven.

TABLE 1. The Ten Discrete Power Levels as Taken From the Fig. 8 Plot

k_{mod}	0.1	0.2	0.3	0.4	0.5	0.6	0.7	0.8	0.9	1
P_{out} $[W]$	5	23	57	114	199	309	359	435	666	1000

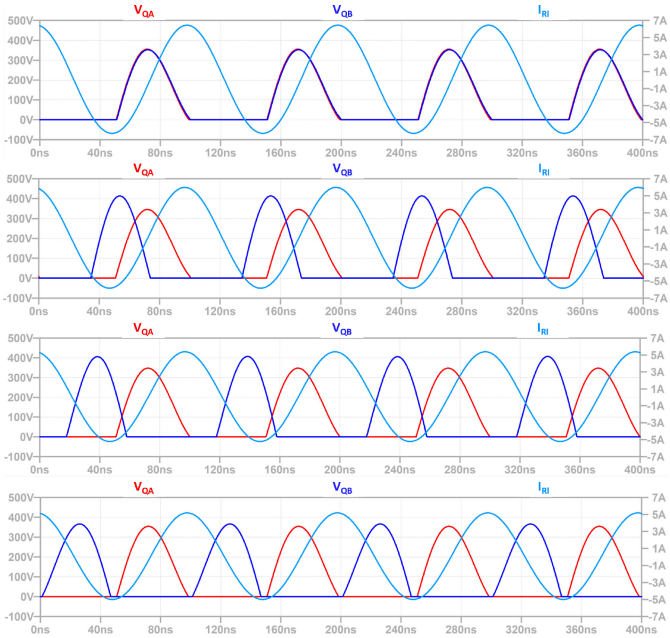

FIGURE 14. A typical drain waveforms across the switches (red = A, blue = B) and load current (light blue) for $[0.9_k, 0.1_r]$ as the phase-shift angle is adjusted from 0 degree to 180 degrees. From top to bottom, $\theta = 0$, 60, 120 and 180 degrees.

Here, we will look at filling the gap between the two highest power cases. At k_{mod} equals to 1, all portions of the circuit operate synchronously as amplifiers and output 1000 W of power. At k_{mod} equals to 0.9, the gate signal is applied to 90% of the circuit, which then operates as amplifiers. The rest of the circuit operates as a passive rectifier, and the output power at this modulation level is 666 W.

With careful observation, we can see that the k_{mod} equals to 1 case is actually the same as what we would get if we use the circuit representation in Fig. 13 with k equals to 0.9, r equals to 0.1 and θ equals to 0 degree $[0.9_k, 0.1_r, 0_\theta]$. More importantly, the k_{mod} equals to 0.9 case is also very similar to the circuit with k equals to 0.9, r equals to 0.1 and θ equals to 180 degrees $[0.9_k, 0.1_r, 180_\theta]$. The only difference is that this 180-degree phase-shifted r portion will operate as an active rectifier, replacing the passive rectifier formed by the diode in the modular "on/off" alone case. However, by controlling the phase of this r unit, its operation can be adjusted from working fully as an amplifier to working fully as a rectifier, as well as anything in between. This means that by adjusting the phase-shift angle, θ, any output power between these two power points can be generated. The same applies to the output power between other adjacent discrete power points.

C. CIRCUIT OPERATION

In order to maintain high efficiency, the active switches need to maintain ZVS conditions across the whole operation range. In this section, we will look at how the phase-shifting control is able to maintain this condition, as well as its output power vs phase relationship. Similar to the previous section on modular "on/off" control, only the two limit cases of k close to 1 and k close to 0 will be analyzed.

1) THE LARGE *k* CASE

For zero-voltage turn-on, the impedance the switch sees has to be inductive enough to discharge the junction capacitance of the switch. Obviously, at $[0.9_k, 0.1_r, 0_\theta]$ (the full power condition), this inductive impedance is already achieved from the way class-E amplifier is tuned. Thus, we have to look at how this inductive impedance is maintained at other phase-shift angles.

Fig. 14 shows typical drain waveforms across the switches Q_A and Q_B as well as the load current I_{Rl} as the control condition is swept from $[0.9_k, 0.1_r, 0_\theta]$ to $[0.9_k, 0.1_r, 180_\theta]$. As the angle increases, the fundamental of the "phase-shift" unit will lead that of the "on" unit more and more. When the angle is less than 90 degrees, the power from both units will combine, resulting in the phase of the output current shifting to the left. When the angle goes above 90 degrees, the "phase-shift" unit will start subtracting power from the "on" unit, causing in the phase of the output current to start shifting back to the right. However, at this high k case, as the power from the "on" unit is much higher than that of the small "phase-shift" unit, this shift of the output phase is insignificant.

From the perspective of the switch Q_B, its voltage will lead the output current more and more as the angle increases. As a result, it sees an increasingly more inductive loading up to the phase angle of 90 degrees. Past this point, the current across the switch becomes negative as it starts converting power back

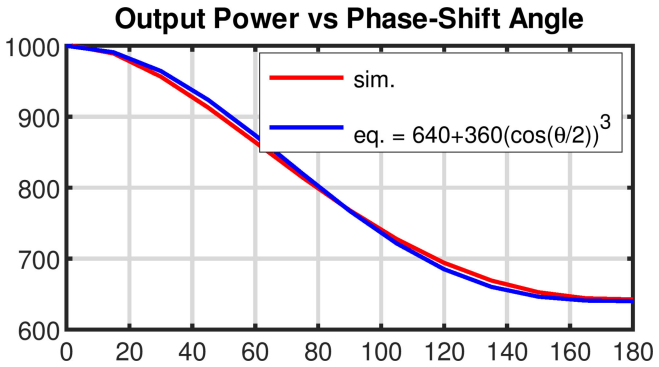

FIGURE 15. Output power [W] (y-axis) vs phase-shift angle θ [deg] (x-axis) relationship for $[0.9_k, 0.1_r, 0_\theta]$ to $[0.9_k, 0.1_r, 180_\theta]$ modulation.

to dc, causing the impedance that the switch sees to begin losing its extra inductive-ness. While this added inductance increases the circulating current and the peak drain voltage of the switch, it also helps the "phase-shifted" circuit to maintain its ZVS condition. Notice that if instead, this r unit was phase-shifted so that it lags the rest of the circuit, the opposite condition with increasingly more capacitive loading would occur and cause this small unit to lose its ZVS.

From the perspective of the switch Q_A, the opposite changes happen. Its voltage maintains a constant phase, but the slight change in the phase of the output current will cause it to see slightly less inductive load as the angle increases. Nonetheless, as this change is minimal, it causes a negligible effect on the ZVS condition of the "on" unit. If the "phase-shift" unit is not much smaller than the rest of the circuit, however, the change in the loading on the "on" unit will be significant, resulting in hard-switching and reduced efficiency.

Fig. 15 shows the change in the output power as the phase-shift angle increases from 0 to 180 degrees. At this end of the k value, the power vs. phase closely follows a cubic of cosine relationship. Unlike in a case of two ideal power sources combining power where a cosine square relationship is expected, this steeper relationship is a result of the extra change in the output power of the "phase-shift" unit due to the extra inductive loading.

2) THE SMALL k CASE

As previously stated, when the k value is approximately less than 0.5, the "off" unit no longer rectifies and operates fully as a resonant tank. Fig. 16 shows typical drain waveforms across the switches Q_A, Q_B and Q_C as well as the load current I_{Rl} as we sweep the control condition from $[0.3_k, 0.1_r, 0_\theta]$ to $[0.3_k, 0.1_r, 180_\theta]$. Because the "on" portion is no longer much larger than the "phase-shift" portion, the shift in the phase of the output current becomes more pronounced.

To the switch Q_B, this causes the increase in the inductive loading due to the phase angle change to be lower than in the large k case. On the other hand, to the switch Q_A, this causes the reduction in the inductive loading due to the phase angle change to be higher than in the large k case. By itself, this

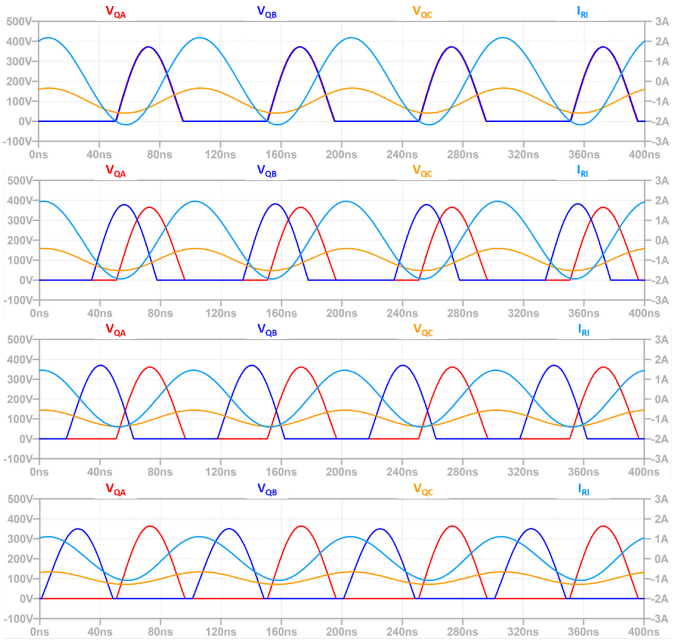

FIGURE 16. A typical drain waveforms across the switches (red = A, blue = B, yellow = C) and load current (light blue) for $[0.3_k, 0.1_r]$ as the phase-shift angle is adjusted from 0 degree to 180 degrees. From top to bottom, θ = 0, 60, 120 and 180 degrees.

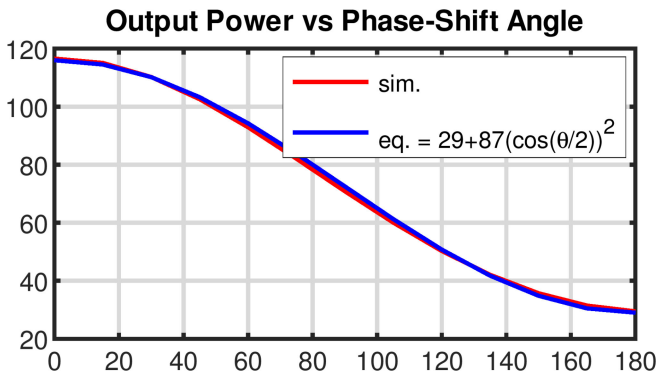

FIGURE 17. Output power [W] (y-axis) vs phase-shift angle θ [deg] (x-axis) relationship for $[0.3_k, 0.1_r, 0_\theta]$ to $[0.3_k, 0.1_r, 180_\theta]$ modulation.

reduction in the inductive loading would result in the switch Q_A of the "on" unit losing its ZVS turn-on. However, from (11), it can be shown that as the k value becomes progressively smaller (the "off" portion becomes increasingly larger), the load impedance presented to the active part of the circuit, Z_k, will become more and more inductive. This inductive impedance counteracts the effect of the phase-shifting on the switch Q_A, allowing both active portions to maintain ZVS.

Fig. 17 shows the change in the output power as the phase-shift angle increases from 0 to 180 degrees. At this end of the k value, the power vs. phase return to closely follow a square of cosine relationship typical of two power sources combining. Because the load is already highly inductive due to the large "off" portion, the extra change in the loading as the angle increases is insignificant and does not affect the circuit as it did in the large k case.

V. COMPARISON WITH OTHER POWER MODULATION METHODS

This section will provide a brief comparison between different power control/modulation methods used in switched-mode amplifiers. The three methods discussed are dc input voltage adjustment, outphasing modulation, and the proposed modular on/off and phase-shifting modulation. The advantages and disadvantages of each method will be explored.

A. DC INPUT VOLTAGE ADJUSTMENT

In this method, an RF amplifier is designed and tuned for a fixed output power. Then, a separate dc-to-dc converter is added in front of the switched-mode amplifier. As the output power of a switched-mode amplifier is proportional to its input voltage, by adjusting the output voltage of the dc-to-dc converter, the eventual output power of the RF amplifier can be adjusted and controlled [34], [35].

The biggest advantage of this power modulation method is its simplicity, allowing for power modulation without requiring any change to the RF amplifier design. Moreover, as the dc voltage decreases, lowering the RF output power, the circulating voltage and current inside the RF amplifier also lower, reducing the amplifier's loss.

One disadvantage of this method is the increased system size due to the extra dc-to-dc converter. Another disadvantage with this method is that its RF power control speed/bandwidth directly depends on the adjustment speed of the dc-to-dc converter output. Typically, this bandwidth will be in the order of 1–10 kHz [36]–[38]. While dc-to-dc converters can be designed to operate at higher switching frequencies to improve their control speed, this comes at the cost of extra loss and reduced efficiency [39]–[41], making this method ill-suited for high-speed high-power power control.

B. OUTPHASING MODULATION

In outphasing, the amplifier circuit is divided into two equal halves, both outputting power. These amplifiers are symmetrically phase-shifted away from each other. Then, a power combiner network is used to combine their outputs. This allows the combined output power to cover the whole power range as the outphasing angle changes from 0 to 180 degrees [19], [20].

One clear benefit of the outphasing method is in its control speed. Depending on how the system is designed and what type of combiner network is used, control bandwidths from 0.5% to 4% of carrier frequencies have been demonstrated [42]–[44]. For a 13.56 MHz RF system, this translates to the bandwidth in the range of 100s of kHz.

A major drawback of this control method is its low system efficiency under light-load condition due to the mismatched portion of the combined power having to be dissipated away [21]. While a lot of research has been done to improve this, efficiency drop between 20-60% at light (10%) load relative to full load is common in outphasing systems [22]–[26].

C. PROPOSED MODULAR ON/OFF AND PHASE-SHIFTING MODULATION

In this proposed technique, the circuit is divided into multiple small units. While they can be of equal size/power, it is best that they are scaled by the power of two such that many discrete power steps can be generated. Due to the way each class-E amplifier is designed and tuned, the power combining capability is intrinsic. Thus, no extra power combiner network is required. To control the output power, two mechanisms are used. The crude power control comes from the turning "on/off" of different numbers of the sub-circuits. Then, the phase-shifting is used on the smallest of these units to cover the gap between the discrete output power levels. While this system is not yet evaluated for dynamic tracking of command signals (which is beyond the scope of this study), simulation and experimental results so far have indicated that the proposed system will have similar bandwidth to that of outphasing systems.

The biggest advantage of this proposed circuit/controller over the outphasing is its improvement in efficiency. In a power combiner based circuit, there are always associated parasitic losses due to non-ideal components in the combining network. By eliminating the need for a power combiner stage, we remove this loss component altogether. This means that our proposed circuit will always achieve higher efficiency at full power than a combiner-based circuit.

Not only that, unlike in outphasing where conduction losses are always present on every sub-circuit even at the low power level, our proposed control method can completely turn off unneeded units at light load by allowing them to operate as simple resonant tanks. When these units are turned off, their associated conduction losses are eliminated, leaving only the parasitic losses in their capacitors and inductors. This causes the proposed circuit to also achieve higher efficiency at light load than that of outphasing circuits.

In contrast, one of the most significant disadvantages of this proposed method is in the output power linearity. Although the output power is also not linearly proportional to the phase angle in an outphasing system, pre-distortion can be used to nullify the issue. While this is also possible in our proposed system, because we have to adjust both the number of the "on/off" units and the phase angle, pre-distortion is made much more difficult.

D. PERFORMANCE COMPARISON

To demonstrate the improved performance over existing technologies, we will compare the efficiency of this new control method with the power combining and outphasing method from Perreault *et al.* [30]. To the best of our knowledge, this is currently the highest performing system that is suitable for high-speed power control. To make for a fair comparison, the same transistor model and passive component quality factors as what Perreault *et al.* had used in [30] to compare his proposed circuit with the Chireix combiner are used.

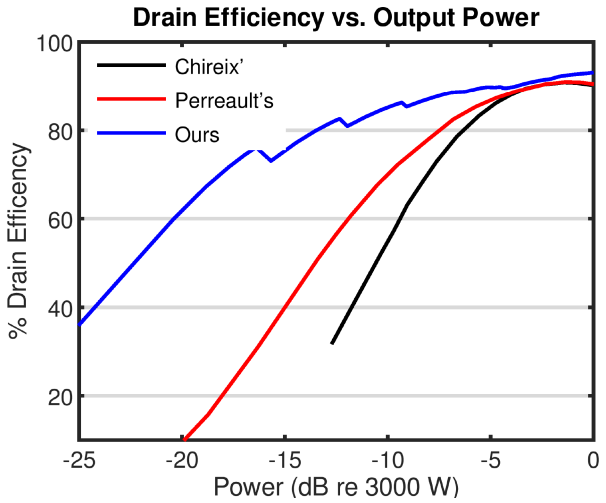

FIGURE 18. A comparison between the efficiency vs output power of our proposed system (blue), Perreault's (red), and Chireix's (black).

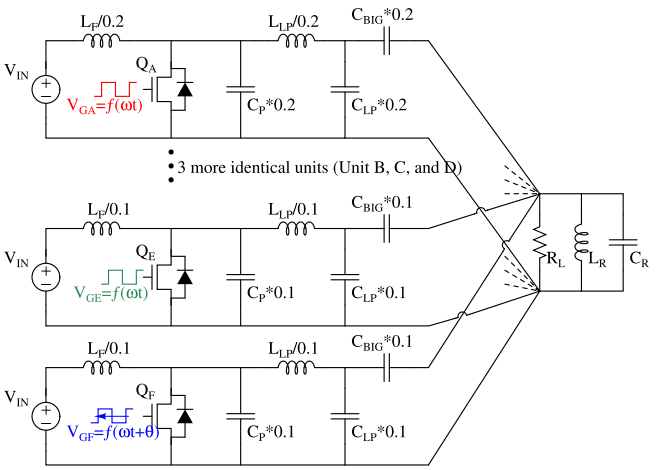

FIGURE 19. Six power-combinable class-E amplifiers circuits directly combining power. Resonant LC filter is employed in parallel to the output load.

To generate 3000 W maximum power, our simulated system consists of 6 power amplifiers combining the output power via the modified low-pass network. The amplifier is tuned according to section II and controlled according to section III and IV. Four of these amplifiers are tuned for 600 W output each, while the other two units are tuned for 300 W. One of the 300 W units is used as a phase-controlled unit. The other units will either be "on" or "off," depending on the output power level. In the k & r notation, $k = 0.1, 0.2, ..., 0.9$ and $r = 0.1$.

Fig. 18 shows the comparison between the simulated drain efficiency of our system vs Perreault's and Chireix's. The steps in our efficiency curve come from the change in the number of units that operate as amplifiers (changing the number k). As the output power is reduced, fewer units are needed. Whenever a unit is taken off, its fixed circulating loss is eliminated, resulting in an increase in efficiency. As seen in this figure, our proposed system shows higher efficiency than both other systems across the whole power range. At 0 dB (full power), our system achieves 3% higher efficiency than that of both Perreault's and Chireix's systems. At -10 dB power, our system shows 85% efficiency vs. 70% in Perreault's and 55% in Chireix's. At -20 dB power, our system shows 62% efficiency vs. 8% in Perreault's (Chieix's is not longer operatable at this lower power level).

VI. EXPERIMENTAL DEMONSTRATION

This section will experimentally demonstrate the design of a 13.56 MHz 1500 W power-combinable class-E amplifier utilizing the proposed modular "on/off" and phase-shifting control technique. The intended application of this amplifier is for high-speed multi-level pulsing, which can be used for plasma generation in semiconductor processing industries [16]–[18].

TABLE 2. Operating Condition and Component Values of the Simulated Power-Combinable Class-E Amplifier Circuits in Fig. 19

V_{in} [V]	FET [GS]	L_f [nH]	C_p [pF]	L_{lp} [nH]	C_{lp} [pF]	L_r [nH]	C_r [pF]	C_{big} [nF]	R_l [Ω]
100	66504B/02B	73.3	875	242	568	169	704	10	50

A. CIRCUIT DESIGN

To simplify the prototyping process and help spread out the heating, six circuits combining power with four units tuned for 300 W and two units tuned for 150 W are used. Again, in the k & r notation, $k = 0.1, 0.2, ..., 0.9$ and $r = 0.1$. To get the best performance at this high frequency, 650 V GaN transistors from GaNSystems as the main power switches are used. To optimize the circuit efficiency in the face of "off-state" C_{oss} loss in GaN devices, the device size and the input voltage are chosen according to [45], [46].

Fig. 19 shows the schematic of the circuit used in this prototype. In this schematic, the unit A to D are the 300 W units, and the unit E and F are the 150 W units. Unlike in Fig. 13, here we use a single parallel resonant filter at the output instead of six separate series resonant filter along the pre-combined branches. This is done to reduce the overall component count and final size/volume of the circuit. To still maintain the dc isolation, dc-blocking capacitors, C_{big}(s), are also added to the circuit.

The general design step follows that outlined in section II. However, to take into account losses in the switches and passive components, the circuit is tuned using the equation for 1600 W power instead of the nominal 1500 W. Minor adjustment is then made on simulation to achieve the optimal performance.

Table 2 summaries the component values used in the simulation. For the simulation, a quality factor of 200 is used for the input inductors, L_f(s), and a quality factor of 400 is used

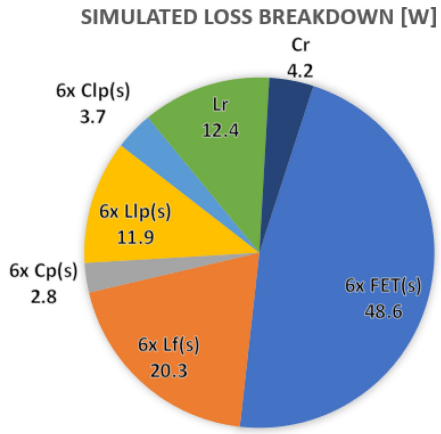

FIGURE 20. The simulated loss breakdown of the amplifier shown in Fig. 19 when operates at full output power.

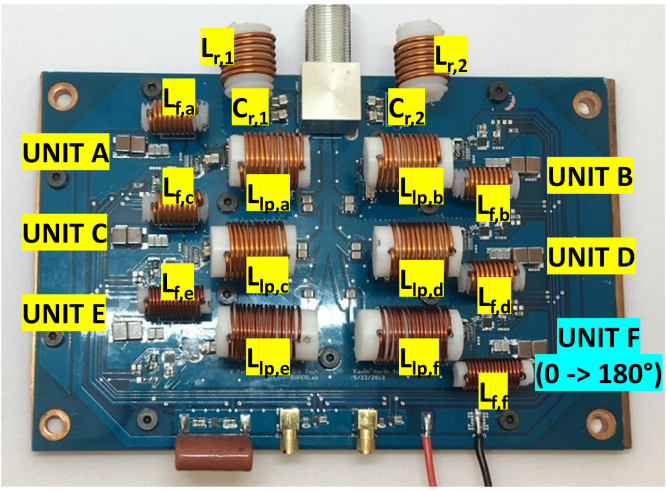

FIGURE 21. The 1500 W 13.56 MHz amplifier circuit with modular "on/off" and phase-shifting control. The parallel resonant filter at the output is split into two halves for symmetry. The board dimension is 195 × 125 mm.

for all of the other inductors. A quality factor of 1000 is used for all of the capacitors.

According to the simulation, the circuit is expected to have a dc-to-RF efficiency of 93.7% at the maximum output power of 1530 W. Fig. 20 shows the simulated loss breakdown across the different components at this maximum power level. To accurately predict the losses, the C_{oss} losses of the GaN transistors are also included in the simulation using the equations from [47].

B. EXPERIMENTAL RESULTS

Shown in Fig. 21, the actual circuit is implemented on a standard 4-layer FR-4 PCB using the component values from the simulation. Five of the sub-circuits (unit A to E) share the same gating signal from one channel of a two-channel signal generator. AND logic gates are used to buffer these signals into each unit, as well as allowing us to separately enable/disable each unit to perform the modular on/off control. The "phase-shift" unit (Unit F) receives its gating signal from the second channel of the signal generator, which allows us to arbitrarily control its phase. All of the inductors are air-cored and hand-wound. 12 AWG copper magnet wires are used for the L_f(s) and L_{lp}(s) of the unit A to D, as well as for the L_r(s). 16 AWG copper magnet wires are used for the L_f(s) and L_{lp}(s) of the unit E and F. This smaller diameter wire allows us to maintain roughly the same volume of the inductors in the lower power units as those in the higher power units. Low loss C0G ceramic capacitor from American Technical Ceramic (ATC) are used for C_p(s) C_{lp}(s) and C_r(s). Due to the high operating frequency, parasitic inductance and capacitance of the PCB traces can affect the tuning and are also taken into account.

GS66504B(s), 100 mΩ 650 V GaN transistors, are used as the main switches in unit A to D. Another GaN device in the same series but with half the die size, GS66502B(s), 200 mΩ 650 V GaN transistors, are used in unit E and F. To sufficiently drive the gate of the tested GaN HEMTs, low-side gate drivers, LM5114 from Texas Instruments, are used. We place the gate drivers as close as possible to the GaN switches to minimize the loop inductance in the gate and use a gate resistor of 2.4 Ω to dampen any ringing in the gate voltage. Additionally, SiC Schottky diodes STPSC406 from ST Microelectronics are added in parallel to the switches to reduce the loss associated with reverse conduction in GaN transistor [48].

To facilitate the cooling of the switching devices, we make a custom copper heat spreader with six small posts that directly contact the thermal pad of the GaN transistors via 3.5 mm drill holes directly under the devices. Water cooling, which is standard for commercial RF systems at this power level, is also used.

The input power is calculated from the dc input voltage and current under continuous operation. The input voltage is measured with a digital multimeter, Agilent 34411A, and the input current is recorded from the readout of the dc power supplies, Agilent N5767A(s). The output power into the 50 Ω load is measured with a directional coupler/ power meter setup. The setup consists of a calibrated 4-port RF directional coupler, C5827-10, from Werlatone Inc., two N8482A thermocouple power sensors from Keysight Technologies, and an N1914A EPM series power meter from Keysight Technologies.

Fig. 22 shows the measured drain waveforms on all six subcircuits, as well as the output voltage waveform at three different power levels achieved with the proposed control method. In Fig. 22(a), since the full power of the circuit is slightly too high, to get exactly 1500 W, unit F is adjusted to 20-degree phase-shift while all the other units are "on" $[0.9_k, 0.1_r, 20_\theta]$. In Fig. 22(b), unit E (the 10% unit) is turned "off," and at this power level, it operates as a rectifier. To get 800 W, unit F is adjusted to 55-degree phase-shift while the rest of the units are "on" $[0.8_k, 0.1_r, 55_\theta]$. In Fig. 22(c), which is the light load case, only the unit A (the 20% unit) and unit E (the 10% unit) are "on." To get 100 W, unit F is adjusted to 43-degree phase-shift, and the rest of the units are "off" $[0.3_k, 0.1_r, 43_\theta]$.

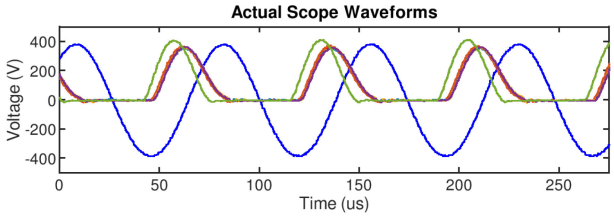

(a) Output power = 1500 W. Unit A, B, C, D and E = "on." Unit F = 20 deg "phase-shifted."

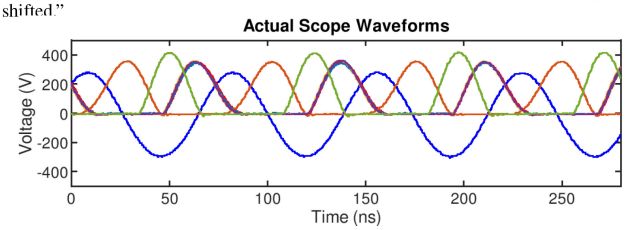

(b) Output power = 800 W. Unit A, B, C and D = "on." Unit E = "off." Unit F = 55 deg "phase-shifted."

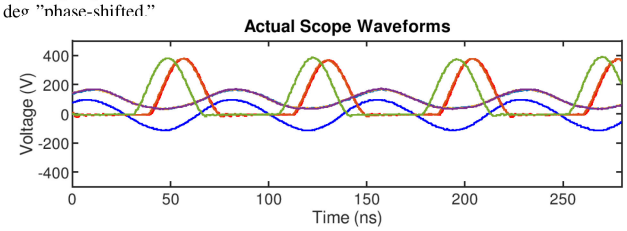

(c) Output power = 100 W. Unit A and E = "on." Unit B, C, and D = "off." Unit F = 43 deg "phase-shifted."

FIGURE 22. The experimentally measured waveforms of the circuit operating at three different output power level. Waveforms from each half (left/right) of the circuit along with the output voltage are captured on a 4-channel oscilloscope. Then, they are combined and plotted together via MATLAB. (Output voltage = blue, Drain A = red, Drain B = magenta, Drain C = light blue, Drain D = yellow, Drain E = orange, Drain F = green).

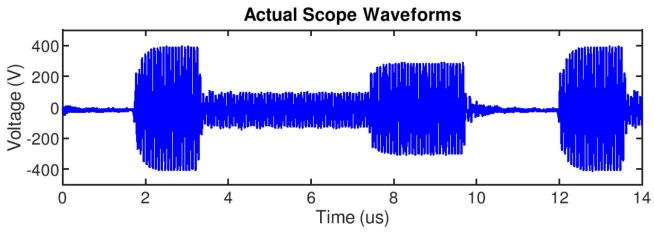

FIGURE 23. The experimentally measured output voltage waveform under multi-level pulsing operation. Waveform is captured on an oscilloscope then plotted via MATLAB.

Fig. 23 shows the measured output voltage waveform under multi-level pulsing operation achieved with the proposed control method. The three power levels in order are 1500 W (15% duty cycle), 100 W (40% duty cycle), and 800 W (23% duty cycle). The pulsing frequency is 100 kHz. From the experimental waveform, a very fast transient time of less than 0.5 μs (approximately 7 cycles) is observed at each power transition.

Fig. 24 compares the experimentally measured and simulated dc-to-RF efficiency achieved with the proposed control method. The measurement results are in very good agreement with the simulation. From the plot, the circuit achieves 93%

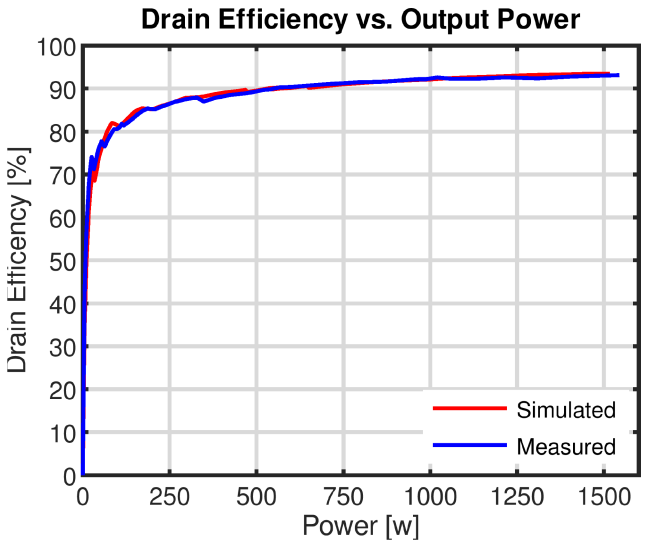

FIGURE 24. The experimentally measured and simulated efficiency vs output power. The dc input voltage is fixed at 100 V while the "on/off" of different units and "phase-shifting" of unit F is used to adjust the output power.

efficiency at the full rated power of 1500 W, maintains above 90% efficiency down to half the rated power of 750 W, and continues to have above 80% efficiency all the way down to 100 W.

VII. CONCLUSION

This paper describes a new high-speed power control method for power-combinable class-E amplifiers. In power-combinable class-E amplifiers, power from multiple amplifiers can be directly combined without the need for an extra power combiner network. When used in conjunction with this proposed power control technique, the full range (from zero to maximum) of output power can be generated with no modification to the circuit needed.

This power control technique utilizes two mechanisms, the modular on/off and the phase-shifting control. In modular on/off, a different number of sub-circuits are turned "on/off" to crudely control the output power. In phase-shifting, the smallest sub-circuit of the whole system is phase-shifted away from the rest of the circuit to finely adjust the output power. The two mechanisms work in conjunction to maintain ZVS conditions across all active switches while allowing arbitrary output power to be generated.

The benefits of this control method include the simplicity of the design and the reduction in the number of components needed, as well as the increased phase-angle-to-output-power resolution. However, the biggest advantage this proposed control method has over the existing outphasing control technique is the boost in dc-to-RF conversion efficiency across the whole power range. At full load, the elimination of the power combiner network reduces parasitic loss associating with it, allowing the proposed system to achieve higher efficiency

than a combiner-based system. At light load, the ability to completely turn off some of the subcircuits heavily increases the circuit's efficiency.

This proposed amplifier system's performance is first compared via circuit simulation with existing outphasing amplifier systems, then demonstrated with an actual circuit implementation. In particular, we demonstrated a 13.56 MHz RF amplifier with the ability to generate any output power level from zero to 1500 W without changing the input voltage. The circuit has 20 W/in^3 power density, attains 93% dc-to-RF efficiency at 1500 W (full load), and maintains above 83% efficiency down to 150 W (10% load). This achieved efficiency both at full load and light load are much higher than that of other studies at similar frequency (79/39% @ 100/10 W – 27.12 MHz [42], 83/23% @ 20/2 W – 48 MHz [49]). Furthermore, the circuit achieves a transient time of less than 0.5 μs (7 cycles) when switching from one power level to another.

ACKNOWLEDGMENT

The authors would like to thank DAIHEN Corporation for their support in this project through the funding provided to the Stanford SUPERLab.

REFERENCES

[1] S. Zhukov and V. Kozyrev, "Push-pull switching generator without switching loss," *Poluprovodnikovye Pribory v Tekhnike Elektrosvyazi*, vol. 15, pp. 95–107, 1975.
[2] D. C. Hamill, "Impedance plane analysis of class DE amplifier," *Electron. Lett.*, vol. 30, no. 23, pp. 1905–1906, 1994.
[3] S.-A. El-Hamamsy, "Design of high-efficiency RF class-D power amplifier," *IEEE Trans. Power Electron.*, vol. 9, no. 3, pp. 297–308, May 1994.
[4] N. O. Sokal and A. D. Sokal, "Class E-a new class of high-efficiency tuned single-ended switching power amplifiers," *IEEE J. Solid-State Circuits*, vol. 10, no. 3, pp. 168–176, Jun. 1975.
[5] N. O. Sokal and A. Mediano, "Redefining the optimum RF class-E switch-voltage waveform, to correct a long-used incorrect waveform," in *Proc. IEEE MTT-S Int. Microw. Symp. Dig.*, Jun. 2013, pp. 1–3.
[6] V. Tyler, "A new high-efficiency high-power amplifier," *Marconi Rev.*, vol. 21, no. 130, pp. 96–109, 1958.
[7] F. H. Raab, "Class-F power amplifiers with maximally flat waveforms," *IEEE Trans. Microw. Theory Technol.*, vol. 45, no. 11, pp. 2007–2012, Nov. 1997.
[8] K. Honjo, "A simple circuit synthesis method for microwave class-F ultra-high-efficiency amplifiers with reactance-compensation circuits," *Solid-State Electron.*, vol. 44, no. 8, pp. 1477–1482, Jun. 2000.
[9] S. D. Kee, I. Aoki, A. Hajimiri, and D. Rutledge, "The class-E/F family of ZVS switching amplifiers," *IEEE Trans. Microw. Theory Technol.*, vol. 51, no. 6, pp. 1677–1690, Jun. 2003.
[10] J. W. Phinney, D. J. Perreault, and J. H. Lang, "Radio-frequency inverters with transmission-line input networks," *IEEE Trans. Power Electron.*, vol. 22, no. 4, pp. 1154–1161, Jul. 2007.
[11] J. M. Rivas, Y. Han, O. Leitermann, A. Sagneri, and D. J. Perreault, "A high-frequency resonant inverter topology with low voltage stress," in *Proc. IEEE Power Electron. Specialists Conf.*, 2007, pp. 2705–2717.
[12] L. Gu, G. Zulauf, Z. Zhang, S. Chakraborty, and J. Rivas Davila, "Push-pull class Φ_2 RF power amplifier," *IEEE Trans. Power Electron.*, p. 1, Oct. 2020.
[13] A. Agarwal, P. J. Stout, S. Banna, S. Rauf, K. Tokashiki, J.-Y. Lee, and K. Collins, "Effect of simultaneous source and bias pulsing in inductively coupled plasma etching," *J. Appl. Phys.*, vol. 106, no. 10, 2009, Art. no. 103305.
[14] D. J. Economou, "Pulsed plasma etching for semiconductor manufacturing," *J. Physics D: Appl. Physics*, vol. 47, no. 30, 2014, Art. no. 303001.
[15] V. M. Donnelly and D. J. Economou, "Atomic layer etching with pulsed plasmas," U.S. Patent Appl. 12/966,844, Jun. 2011
[16] J. Shoeb, A. Paterson, and Y. Wu, "Multi-level parameter and frequency pulsing with a low angular spread," U.S. Patent Appl. 10,224,183, Mar. 2019.
[17] J. Shoeb, A. Paterson, and Y. Wu, "Multi-level pulsing of DC and RF signals," U.S. Patent Appl. 10,304,660, May 28, 2019.
[18] D. Shimizu, W. Lee, K. Kawasaki, L. Ling, P. Justin, and K. Choi, "Smart multi-level RF pulsing methods," U.S. Patent Appl. 9,872,373, Jan. 16, 2018.
[19] H. Chireix, "High power outphasing modulation," *Proc. Inst. Radio Eng.*, vol. 23, no. 11, pp. 1370–1392, Nov. 1935.
[20] D. Cox, "Linear amplification with nonlinear components," *IEEE Trans. Commun.*, vol. 22, no. 12, pp. 1942–1945, 1974.
[21] F. H. Raab *et al.*, "RF and microwave power amplifier and transmitter technologies-part 1," *High Freq. Electron.*, vol. 2, no. 3, pp. 22–36, 2003.
[22] R. Langridge, T. Thornton, P. M. Asbeck, and L. E. Larson, "A power re-use technique for improved efficiency of outphasing microwave power amplifiers," *IEEE Trans. Microw. Theory Technol.*, vol. 47, no. 8, pp. 1467–1470, Aug. 1999.
[23] X. Zhang, L. E. Larson, P. M. Asbeck, and R. A. Langridge, "Analysis of power recycling techniques for RF and microwave outphasing power amplifiers," *IEEE Trans. Circuits Syst. II: Analog Digital Signal Process.*, vol. 49, no. 5, pp. 312–320, May 2002.
[24] P. A. Godoy, D. J. Perreault, and J. L. Dawson, "Outphasing energy recovery amplifier with resistance compression for improved efficiency," *IEEE Trans. Microw. Theory Technol.*, vol. 57, no. 12, pp. 2895–2906, Dec. 2009.
[25] H. Chireix, "High power outphasing modulation," in *Proc. Inst. Radio Eng.*, vol. 23, no. 11, 1935, pp. 1370–1392.
[26] I. Hakala, D. K. Choi, L. Gharavi, N. Kajakine, J. Koskela, and R. Kaunisto, "A 2.14-GHz Chireix outphasing transmitter," *IEEE Trans. Microw. Theory Technol.*, vol. 53, no. 6, pp. 2129–2138, 2005.
[27] W. Gerhard and R. Knoechel, "Improved design of outphasing power amplifier combiners," in *Proc. German Microw. Conf.*, 2009, pp. 1–4.
[28] R. Beltran, F. H. Raab, and A. Velazquez, "HF outphasing transmitter using class-E power amplifiers," in *Proc. IEEE MTT-S Int. Microw. Symp. Dig.*, 2009, pp. 757–760.
[29] T. Ni and F. Liu, "A new impedance match method in serial Chireix combiner," in *Proc. Asia-Pacific Microw. Conf.*, 2008, pp. 1–4.
[30] D. J. Perreault, "A new power combining and outphasing modulation system for high-efficiency power amplification," *IEEE Trans. Circuits Syst. I: Reg. Papers*, vol. 58, no. 8, pp. 1713–1726, Aug. 2011.
[31] K. Surakitbovorn and J. M. Rivas-Davila, "A simple method to combine the output power from multiple class-E power amplifiers," *IEEE J. Emerg. Sel. Topics Power Electron.*, pp. 1–1, 2020.
[32] M. Acar, A. J. Annema, and B. Nauta, "Analytical design equations for class-E power amplifiers," *IEEE Trans. Circuits Syst. I: Reg. Papers*, vol. 54, no. 12, pp. 2706–2717, Dec. 2007.
[33] D. C. Hamill, "Time reversal duality and the synthesis of a double class E dc-dc converter," in *Proc. 21st Annu. IEEE Conf. Power Electron. Specialists.*, 1990, pp. 512–521.
[34] A. Grebennikov, N. Sokal, and M. Franco, *Switchmode RF Power Amplifiers*. Oxford, U.K.: Newnes, 2011.
[35] F. H. Raab *et al.*, "Power amplifiers and transmitters for RF and microwave," *IEEE Trans. Microw. Theory Technol.*, vol. 50, no. 3, pp. 814–826, 2002.
[36] K. Yao, Y. Meng, and F. C. Lee, "Control bandwidth and transient response of buck converters," in *Proc. IEEE 33rd Annu. Power Electron. Specialists Conf. (Cat. No. 02CH37289)*, vol. 1, 2002, pp. 137–142.
[37] T. Mishima, Y. Ooue, Y. Fukumoto, and M. Nakaoka, "A secondary-side phase-shifting ZVS-PWM dual full bridge dc-dc front-end converter for plasma RF power generator," in *Proc. Int. Conf. Elect. Mach. Syst.*, 2009, pp. 1–6.
[38] T. Mishima, Y. Ooue, Y. Fukumoto, and M. Nakaoka, "An active rectifier-phase shifted ZVS-PWM dc-dc converter with HF planar transformer-link for RF plasma power generator," in *Proc. Int. Conf. Power Electron. Drive Syst.*, 2009, pp. 712–717.

[39] S. Sakata *et al.*, "An 80MHz modulation bandwidth high efficiency multi-band envelope-tracking power amplifier using GaN single-phase buck-converter," in *Proc. IEEE MTT-S Int. Microw. Symp.*, 2017, pp. 1854–1857.

[40] P. Midya, K. Haddad, L. Connell, S. Bergstedt, and B. Roeckner, "Tracking power converter for supply modulation of RF power amplifiers," in *Proc. 32nd Annu. Power Electron. Special. Conf. (IEEE Cat. No. 01CH37230)*, vol. 3, 2001, pp. 1540–1545.

[41] P. Cheng, M. Vasić, O. Garcia, J. Oliver, P. Alou, and J. Cobos, "Design of envelope amplifier based on interleaved multiphase buck converter with minimum time control for RF application," in *Proc. IEEE Energy Convers. Congr. Expo.*, 2011, pp. 1279–1283.

[42] A. S. Jurkov, L. Roslaniec, and D. J. Perreault, "Lossless multiway power combining and outphasing for high-frequency resonant inverters," *IEEE Trans. Power Electron.*, vol. 29, no. 4, pp. 1894–1908, 2013.

[43] J. R. McFarland and T. W. Barton, "Bandwidth of transmission-line resistance compression networks for microwave outphasing transmitters," in *Proc. Texas Symp. Wireless Microw. Circuits Syst.*, 2015, pp. 1–4.

[44] S. Chung, R. Ma, K. H. Teo, and K. Parsons, "Outphasing multi-level RF-PWM signals for inter-band carrier aggregation in digital transmitters," in *Proc. IEEE Radio Wireless Symp.*, 2015, pp. 212–214.

[45] K. Surakitbovorn and J. R. Davila, "Evaluation of GaN transistor losses at MHz frequencies in soft switching converters," in *Proc. IEEE 18th Workshop Control Model Power Electron.*, Jul. 2017, pp. 1–6.

[46] K. N. Surakitbovorn and J. M. Rivas-Davila, "On the optimization of a class-E power amplifier with GaN HEMTs at megahertz operation," *IEEE Trans. Power Electron.*, vol. 35, no. 4, pp. 4009–4023, Apr. 2020.

[47] G. Zulauf, Z. Tong, J. D. Plummer, and J. M. Rivas Davila, "Active power device selection in high- and very-high-frequency power converters," *IEEE Trans. Power Electron.*, pp. 1–1, 2018.

[48] S. Park and J. Rivas-Davila, "Power loss of GaN transistor reverse diodes in a high frequency high voltage resonant rectifier," in *Proc. IEEE Appl. Power Electron. Conf. Expo.*, 2017, pp. 1942–1945.

[49] P. A. Godoy, D. J. Perreault, and J. L. Dawson, "Outphasing energy recovery amplifier with resistance compression for improved efficiency," *IEEE Trans. Microw. Theory Techn.*, vol. 57, no. 12, pp. 2895–2906, Dec. 2009.